

**NOTICE: THIS
MATERIAL MAY
BE PROTECTED
BY COPYRIGHT
LAW (TITLE 17
U.S. CODE).**

Analysis of human lung morphometric data for stochastic aerosol deposition calculations

This article has been downloaded from IOPscience. Please scroll down to see the full text article.

1985 Phys. Med. Biol. 30 541

(<http://iopscience.iop.org/0031-9155/30/6/004>)

View [the table of contents for this issue](#), or go to the [journal homepage](#) for more

Download details:

IP Address: 170.140.250.69

The article was downloaded on 13/07/2012 at 19:54

Please note that [terms and conditions apply](#).

Analysis of human lung morphometric data for stochastic aerosol deposition calculations

László Koblinger† and Werner Hofmann‡

† Central Research Institute for Physics, PO Box 49, H-1525 Budapest, Hungary

‡ University of Salzburg, Erzabt-Klotz str 11, A-5020 Salzburg, Austria

Received 17 September 1984, in final form 23 November 1984

Abstract. A stochastic lung model is proposed for aerosol deposition calculations. Airway geometry is selected randomly to reflect intrasubject variations in the human airway system. This may also be adjusted to take intersubject variations into account. The statistical analysis of the human airway geometry used is based on morphometric data measured at the Lovelace Inhalation Toxicology Research Institute. Average values and distributions of airway diameters and lengths, distributions of branching angles and criteria for termination of the pathway (when the alveolar region is reached) are presented. Correlations between the cross sections of tubes of succeeding generations and those between diameters and lengths of the same generation are also given.

1. Introduction

Current models of inhaled particle deposition in the human respiratory tract make use of stylised forms which are approximations of the real anatomical structure of the lung (Weibel 1963, Horsfield *et al* 1971, Yeh and Schum 1980). Successive generations of air passages are represented by straight cylindrical tubes of specified diameters and lengths, with branching at fixed angles into distal tubes.

The parameters defined in these so-called deterministic models have been derived by averaging data on lung dimensions obtained from various lung casts. Thus each individual lung is described by the same anatomical structure. Evaluations of particle deposition in the respiratory tract from inhalation experiments and model calculations with monodisperse aerosols have shown significant intersubject as well as intrasubject variabilities of total deposition (Lippmann and Albert 1969; Heyder *et al* 1978, 1980; Chan and Lippmann 1980; Tarroni *et al* 1980; Stahlhofen *et al* 1981; Yu and Diu 1982). Current lung models do not, however, reflect the variability of the structural components of the lung which lead to these observed random variations of particle deposition. The first attempts to consider the variability of airway structure were made by Soong *et al* (1979) and Yu *et al* (1979). These authors represented airway lengths and diameters by log-normal probability density functions.

Like Weibel's model A (1963) most lung models are symmetrical, thereby enormously facilitating aerosol deposition calculations. Models which incorporate branching asymmetry, i.e. branching into a major and a minor branch with different lengths, diameters and branching angles, should lead to more realistic predictions (Horsfield and Cumming 1968, Horsfield *et al* 1971, Yeh and Schum 1980). This paper aims to

develop a stochastic lung model for Monte Carlo deposition calculations that incorporates parameter variability as well as asymmetric branching.

2. Structure of the bronchial tree

The airways from the trachea to the alveolar sacs form a structure similar to the crown of a tree; the airways multiply in number toward the periphery. The tree of the human airway system can be described as a sequence of irregular dichotomies (Weibel 1963), i.e. the two conjugate (daughter) elements following a parent tube have different diameters and lengths. There is also a difference in the branching angles; in general the larger daughter deviates less from the direction of the parent.

For the classification of the bronchial tree two basically different numbering methods can be used (Horsfield 1974). The first way is to count down the tree by generations. In this case the trachea is identified by 1 (for example, Phalen *et al* 1978) or by 0 (for example, Weibel 1963) and the generation number is increased by one at every bifurcation. The second way is to count up the tree from the periphery towards the trachea. Here the problem arises of how to continue the numbering if two daughters with different generation numbers meet at their common parent: the method proposed by Horsfield and Cumming (1968) is to give the parent tube a generation number one greater than that of the daughter with the larger generation number.

There are difficulties in the application of either of the two numbering methods. The application of the counting down method is quite straightforward and simple, but since the different alveolar regions can be reached along different paths via markedly varying numbers of bifurcations, a tube after, say, 14 bifurcations may, in one airway path, be a respiratory bronchiole connected solely to the alveolar regions, but in another airway path it may be a bronchus still leading to other bronchi. Thus tubes with different biological functions are identified by the same generation number.

A method for handling these problems has been proposed by Yeates and Aspin (1978) who derived an algorithm for the calculation of total pathway lengths in the Horsfield model; the bronchial tree is structured into large airways, a 1-4 branching zone (where the generation number exceeds the number of the parent by 1 for the major daughter and by 4 for the minor one), a transitional zone (1-3, 1-2) and a symmetric zone (the generation number of both daughters is higher by one than that of the parent). Although branchings 1-4, 1-3, etc could also be found in our data base, the statistical analysis does not confirm the existence of such clearly separated zones.

If the upward numbering is applied then the main difficulty is to find the starting points '... because it was not possible to start counting at the most distal branch ...' (Horsfield 1974). Horsfield and Cumming (1968) designated the first tube with diameter 0.7 mm or less as 'lobula', and generation (or division) number 1 was arbitrarily given to the first tubes with a diameter equal to or higher than 0.7 mm at any pathway.

Partly to avoid this arbitrary selection of starting point and mainly due to lack of peripheral tube data in the morphometric data files we had analysed (see § 4) we decided it might be preferable to use the downward counting method, identifying the trachea by generation number 1. (Generation numbers cited from papers where the trachea is identified by 0 have all been transposed in this paper.) The problem of assigning the same number to tubes with different functions as mentioned above is then considered in the detailed stochastic airway selection procedure described in the next section.

3. Random selection of airways

Geometrical parameters of airways are subject to large random variations. Since the number of the branches in a human respiratory system is extremely high, it is impossible to follow separately each possible pathway of inhaled aerosols. Instead, our intention is to use a Monte Carlo method, i.e. to select pathways randomly but in accordance with the distributions of variables and the correlations found between them.

The variations of the data originate physically from two sources: intersubject and intrasubject variations. To our knowledge there are insufficient published data to carry out an analysis of intersubject variations with any degree of confidence. The intrasubject variations, distributions and correlations of the parameters are discussed in §§ 5–7.

If the statistics are known a random selection method for inspiration can be built up and used for aerosol deposition and radiation dose calculation (Hofmann *et al* 1984) in the following steps.

(1) Select inhaled aerosol diameter and initial velocity. Set time to $t=0$. Set the generation number k to 1.

(2) Select a diameter d_k from the distribution which is representative of the diameters in generation k .

(3) Select the length of the tube l_k from the distribution of the lengths in generation k , taking into account the correlation between the diameters and lengths of tubes in generation k .

(4) Select the diameters of the two daughter tubes d_{k+1}^1 and d_{k+1}^2 from the distributions of the cross section ratios of the parent tube to the daughter tubes and of the minor to major daughters.

(5) Select the lengths l_{k+1}^1 and l_{k+1}^2 from the diameters and the correlation between the diameters and lengths in generation $k+1$.

(6) Select branching angles of the two daughters from the appropriate distributions. Select the gravity angles.

(7) Select the way the aerosol goes on after branching from the diameters, branching angles and laws of flow, then calculate the airflow velocity valid for the way selected.

(8) Calculate the probability of deposition in the investigated tubes and the elapsed time since leaving the last branching and modify the velocity of the aerosol particle.

(9) Decide from the diameter of the daughter tube and the generation number whether the particle has already reached the alveolar region. If so, terminate geometry selection; otherwise let $k = k + 1$, return to step (4) and repeat.

For expiration the same path will be followed in reverse.

As can be seen from the above scheme the physical (deposition) data are calculated analytically and the geometry is selected randomly. We now trace the elapsed time and modify the tube diameters and the air flow velocity in accordance with the breathing cycle. The turning point from inhalation to exhalation is defined by reaching zero velocity, i.e. when inhalation actually ends. This physical termination of the inward movement of the particles stops the cycle of steps (4)–(9).

At the beginning of the bronchial tree, where the number of tubes is very low, it is virtually impossible to find distributions, and the deviations, for example, between parameters of the main bronchi leading respectively to the right and left parts of the lungs, tend to reflect systematic rather than random variations. Therefore, for the first generations actual measured values may even be used; thus, in steps (4)–(6) for low generation numbers (e.g. $2 \leq k \leq 5$) and trivially for steps (2) and (3) ($k=1$) the diameters, lengths and angles are not randomly selected but are assigned values.

4. The data base

To our knowledge, the most detailed morphometric data available are those compiled by Raabe *et al* (1976); other models have been published in their final forms without detailed discussion on the raw data.

Measurements of the geometrical features of human tracheobronchial airways were carried out on silicon rubber replica casts at the Lovelace Inhalation Toxicology Research Institute (ITRI)[†], Albuquerque, NM, USA (Raabe *et al* 1976). All human data measured were stored in 16 files. Table 1 lists these files with the identification numbers subsequently used. The two Caucasian men investigated are designated as A and B.

Table 1. The human lung data sets.

Data set identification no	Original file no	No of tubes measured	Man	Lobe [†]	Cut off criteria [‡]
DS1	1	2667	A	RU	100% to 8 divisions, 25% to 0.8 mm
DS2	3	555	A	RU	10% to terminal
DS3	26	187	A	RU	100% to 3 mm
DS4	2	643	A	RM	100% to 11 divisions, 10% to terminal
DS5	27	77	A	RM	100% to 3 mm
DS6	6	1097	A	RL	100% to 2 mm, 10% to terminal
DS7	28	295	A	RL	100% to 3 mm
DS8	5	1419	A	LU	25% sample, 3/12 major bronchi to 0.8 mm
DS9	29	187	A	LU	100% to 3 mm
DS10	4	1311	A	LL	25% sample, 4/16 major bronchi to 0.8 mm
DS11	30	301	A	LL	100% to 3 mm
DS12	48	121	B	RU	100% to 3 mm
DS13	49	83	B	RM	100% to 3 mm
DS14	50	287	B	RL	100% to 3 mm
DS15	51	195	B	LU	100% to 3 mm
DS16	52	221	B	LL	100% to 3 mm

[†] The first letter in the column denotes: R, right, L, left; the second letter denotes: U, upper, M, middle, L, lower.

[‡] All cut off limits refer to the diameters.

There are cases when more than one data set contains information on the same lobe. In these cases the most important difference is in the 'depth' of preparation, i.e. in the criterion by which the measurements are terminated.

The data recorded were: the length and the diameter of the tube (both with 0.1 mm accuracy); the branching angle (i.e. the angle by which the investigated tube deviates from its parent); the gravity angle (i.e. deviation from the downward vertical axis); and the so-called anomaly codes which indicate if the tube has a significant curvature, grossly non-circular cross section, etc.

The data of any single tube are identified by the line number (record number on the magnetic tape) and, besides the geometrical data and the codes mentioned above,

[†] These data were obtained from 'Research Performed at the Lovelace ITRI', supported by the National Institute of Environmental Health Services under an interagency agreement with the US Energy Research and Development Administration (now DOE), Contract No DE-ACO4-76EV01013.

every line contains two additional numbers showing the location (record number) of the data of its two daughters. By the use of these daughter record numbers, airways can be followed over many generations.

The diameters and lengths are subject to change during the breathing cycle. The values recorded on the Lovelace files refer to the inflated lung. Raabe *et al* (1976) stated that 'the uncast trachea and bronchi have flaccid diameters that may approximate their normal sizes during expiration but the casting material appears to expand them to their normal inspiratory diameters'. Therefore, in the random airway selection procedure, lengths and especially diameters have to be scaled down. A versatile Monte Carlo program permits the use of different scaling amplitudes and different rates of change can be applied even to different diameters.

The cast measurements are terminated for several reasons. 'Complete casts were trimmed to the level of terminal bronchiole' and 'terminal segments on cast... identified... as terminal bronchiole' are marked by code T on the files. There is another code, F, which is assigned to segments 'incomplete, either due to incomplete casting, breakage or trimming' (Phalen *et al* 1978), although 'F code is primarily from trimming' (Yeh 1984). This last comment suggests that segments identified by F codes are mainly terminal segments, especially since there are several tubes coded with both F and T.

In the model every branching is idealised for bifurcations; 'trifurcations or higher order divisions are reduced to two or more bifurcations' (Raabe *et al* 1976). At the bifurcations the daughter with the larger diameter is always considered as the major daughter.

Though this library contains a huge amount of data, it can be seen from the third column of table 1 that the number of tubes measured is large enough for rigorous statistical evaluation in a few data sets only.

5. Diameters in different generations

It is quite plausible and well known from the earliest studies that the cross-sections of the tubes monotonically decrease with increasing generation numbers. For symmetric bifurcations D'Arcy Thompson derived in 1942 the following relation for minimum resistance flow

$$d_n = d_{n-1} 2^{-1/3} \approx 0.794 d_{n-1} \quad (1)$$

where d is the diameter and subscript n is the generation number. (His derivation is nicely repeated in a paper by Horsfield and Cumming 1967.)

The decrease in diameter is demonstrated in figure 1. From the Lovelace ITRI files, DS1, DS8 and DS10 are selected here because these sets contain the largest amount of data and because the cut off criterion is the same in the three cases. For the first five generations we have not plotted values because there are insufficient data to produce reasonable averages. On the other hand, for the tubes with higher generation numbers the diameters are more or less the same for all lobes, but for the first bifurcations asymmetries cannot be handled statistically; they definitely reflect the basic differences between, for example, the right and left parts of the lungs. Therefore, for the first five generations (31 tubes altogether) either the actual measured data can be used, or means and deviations can be extrapolated from the data obtained for higher generations.

For comparison, figure 1 also gives diameters from Weibel's model A (1963), those from the model of Yeh and Schum (1980)—who based their work mainly on the same data as we have—and the theoretical line of equation (1) (d_n fitted to DS1 at $n = 6$).

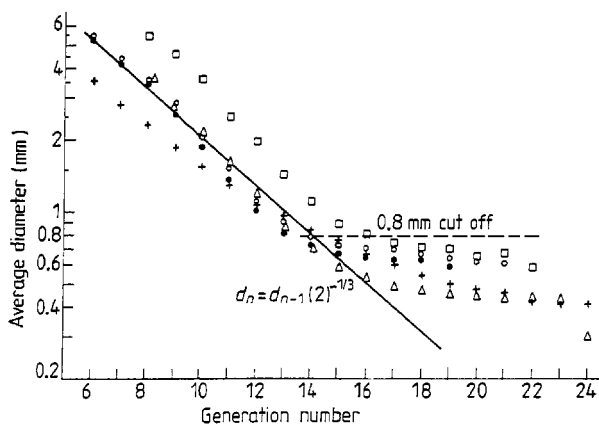


Figure 1. Average airway diameters plotted against generation numbers. (In the comparison of the diameters plotted, especially at higher generation numbers, it should be borne in mind that, in the deterministic models, tubes from any given generation always have the same biological functions, whereas in the real casts analysed the tubes assigned to identical generation numbers are probably not at the same distance from terminal bronchioli. Data from: ●, Lovelace DS1 (right upper lobe); ○, Lovelace DS8 (left upper lobe); □, Lovelace DS10 (left lower lobe); +, Weibel A model (symmetrical); △, Yeh and Schum 1980 (right upper lobe).

The slope of the measured diameters coincides well with the theoretical slope up to about the 14th generation, after which the measured values do not decrease as much as the theoretical slope. The question whether there is a real 'saturation-like' effect or if it is only the cut off of the measurements that leads to an omission of the narrowest tubes needs further analysis.

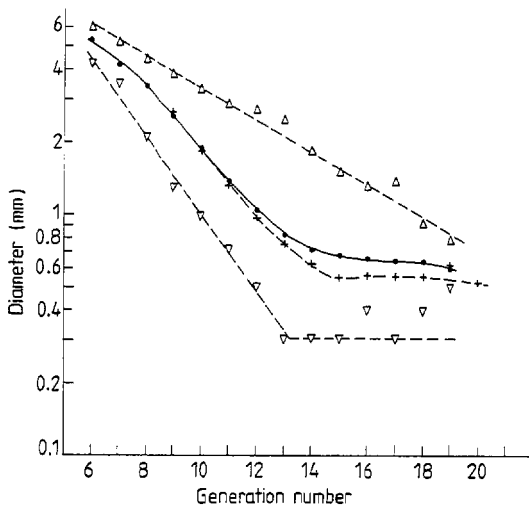


Figure 2. ●, average, △, maximum and ▽, minimum airway diameters for the right upper lobe of man A taken from file DS1. +, average airway diameters taken from file DS2.

In figure 2 average diameters obtained from the same lobe (right upper of man A) with different cut off criteria (see table 1) are compared. (The full and the broken curves are for guidance only.) The data of DS2, where a 10% sample is followed to the terminal, are really lower but the most we can say is that the 'saturation' drifts from the 14th to the 15th generation and the average diameter in generations 15–20 is decreased from about 0.64 to about 0.54 mm.

Table 2. F anomalies in DS2 as a function of generation number.

Generation number	F anomaly (%)
13	2.6
14	27
15	48
16	59
17	53
18	50
19	40

The situation is still doubtful if frequencies of occurrence of the F anomaly codes are investigated. As is seen in table 2 for DS2, at the 13th generation F codes are found in less than 3% of the tubes, but from generation 15 (i.e. just from the 'saturation' point) practically half of the follow-ups are ended because of incomplete casting, breakage or trimming. If we now quite plausibly assume that casting failures and breakages occur more frequently with narrow tubes than with wider ones average diameters may decrease slightly further at even higher generations.

One can also consider the extreme values drawn in figure 2. The maximum diameters registered in different generations of DS1 decrease monotonically and at a quasi-uniform rate in a semi-logarithmic plot for the total investigated range (generations 6-19). There is a similarly constant rate of decrease for the lowest observed diameters but only up to generation 13, where the minimum 0.3 mm is reached and there is no smaller diameter measured. This nature of saturation in the minimum diameters suggests that termination is determined mainly by the diameter of the tubes.

In figure 3(a) the relative frequencies of termination are plotted against the tube diameter, independently of the generation number. Two different curves are obtained if we consider as real termination only those segments which are characterised by the T anomaly code, or the segments also coded by F. (In the former case the F coded tubes are fully neglected from the statistical evaluation.) Since the F code covers mainly cases from trimming but also contributions from incomplete casting and breakage, we can say that the two curves in figure 3(a) are upper and lower limits for termination probabilities at given diameters.

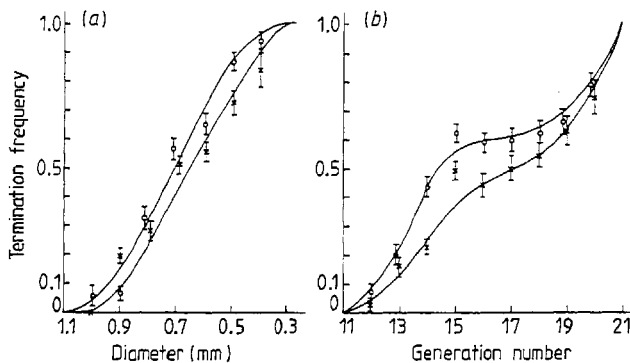


Figure 3. Termination frequencies averaged for all generations of all lobes from files DS2, DS4 and DS6, plotted against (a) diameter and (b) generation number. Termination by: O, F+T codes; and x, T codes.

By a similar analysis the probabilities of termination, i.e. the probabilities of reaching the acini (the region following the terminal bronchioli), can be calculated as a function of the generation number. There is no termination before the 12th generation, and all pathways reach the acini region at generation 21. We can thus calculate the total number of acini N_a by

$$N_a = \sum_{k=12}^{21} 2^{k-1} p_k \prod_{j=11}^{k-1} (1-p_j) \quad (2)$$

where p_k is the probability of termination at generation k ($p_{11}=0$, $p_{21}=1$). Two sets of p_k values are obtained (figure 3b) depending again on whether we accept the F codes or not. If only T coded tubes are considered as terminations, substitution into equation (2) gives about 48 000 for the number of acini, while the acceptance of F results in higher termination probabilities and thus fewer acini—about 20 000. Since this latter figure lies much nearer to the 23 000 estimated by Hansen and Ampaya (1975) from lung cast measurements, we assume that the inclusion of the F coded tubes in the termination investigations leads to less error than their exclusion. However, this decision should later be modified if more accurate measurements become available.

The same type of analysis is then repeated in order to study the influences of both the diameters and the generation numbers on the termination probabilities. In this investigation we involved both the F and T coded tubes as terminal ones. Although the numbers of samples are quite low—and therefore the statistical fluctuations are high—in this double differential distribution, the tendency that the termination probability increases with increasing generation numbers at any fixed diameter is clear. For the stochastic model the use of the following S shaped termination probability p curve set is recommended

$$p = a\{1 + \sin[\pi x^m - (\pi/2)]\} + (0.5 - a)\{1 - \sin[\pi(1-x)^m - (\pi/2)]\} \quad (3)$$

where $x = (1.1 - d)/0.8$, if d is the diameter in mm, and the parameters a and m are functions of the generation number n

$$\left. \begin{aligned} a &= 1.3 - 0.07n \\ m &= 1.03 + 0.324|n - 16.4| \end{aligned} \right\} \quad \text{if } 12 \leq n \leq 17$$

and

$$\left. \begin{aligned} a &= 0 \\ m &= -1.03 + 0.13n \end{aligned} \right\} \quad \text{if } n \geq 18 \quad (4)$$

No termination is assumed to occur before generation 12. The constants in equations (3) and (4) are determined by a weighted least-squares fit; the appropriate weights were derived from the maximum likelihood function of the binomial distribution. In figure 4 the set of termination probability curves calculated using equations (3) and (4) is presented from generations 12 to 20 and an extrapolation is given (broken curve) for generation 30. To demonstrate the goodness of fit we plotted the individual relative frequency data with one standard deviation bars for generations 14 and 18, and their fitted curves are drawn with thicker lines.

The probabilities of equations (3) and (4) can be the basis for the judgement of continuation or termination in step (9) of the procedure in § 3.

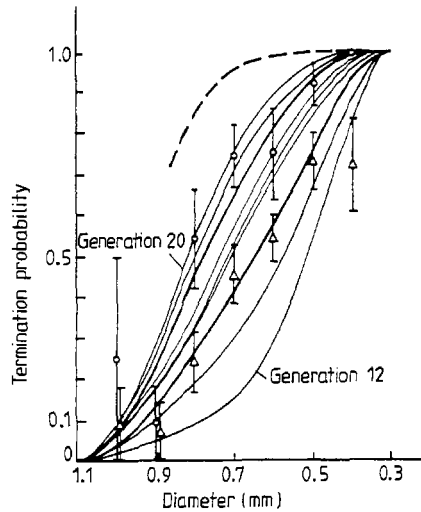


Figure 4. Smooth curve fits to the termination probabilities for generations 12–20. ---, extrapolation for generation 30. Actual termination frequencies are plotted for generations Δ , 14 and \circ , 18. Fits are based on data from files DS2, DS4 and DS6.

6. Distribution of diameters and correlation between parent and daughter tube cross sections

Statistical tests were carried out to check the type of distribution of the data. As is often the case with biological data, diameters were tested against normal and log-normal distributions. According to chi-squared tests the log-normal distribution is more probable for the tube diameters. However, if the data are analysed separately for each data set and each generation, rigorous statistical evaluations do not always confirm the log-normal hypothesis; even so, we believe that in the proposed stochastic model sampling from the log-normal distribution will hardly be the main source of error.

For the actual selections in such cases the easiest method is the selection of the logarithms of the diameters from the normal distribution. For such random selections the averages and the relative standard deviations of the logarithms of the diameters (measured in 0.1 mm units) are given in figures 5(a) and 5(b) respectively.

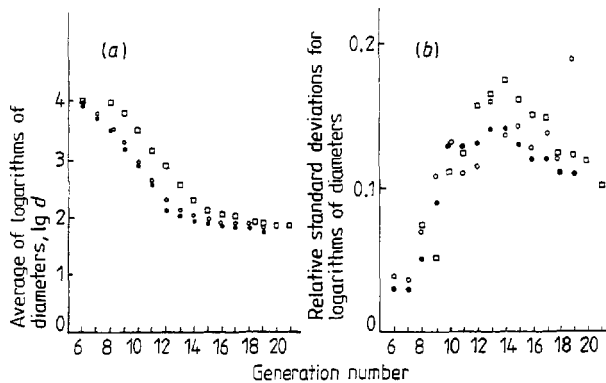


Figure 5. (a) Logarithms of diameters (where d is measured in 0.1 mm units) and (b) their relative standard deviations. Data taken from files: \bullet , DS1; \circ , DS8; and \square , DS10.

Another important question for the random sampling process is whether there is any correlation between the cross sections of the parents and the daughter tubes, i.e. if the parent has a relatively large diameter in its own generation, does it mean that its daughters have large diameters as well (in terms of their own generation)?

From the theoretical derivation mentioned in relation to equation (1), it simply follows that for symmetrical branching and circular tubes the relation

$$\frac{1}{2}A_n/A_{n+1} = 2^{-1/3} \approx 0.794 \quad (5)$$

holds, where A denotes the cross section of the tube ($A = d^2\pi/4$).

Earlier, Horsfield and Cumming (1967) investigated the validity of equation (5) for real—therefore asymmetric—branchings. After measuring 116 bifurcations they obtained an average cross section ratio of 0.88 (very close to the theoretical value of 0.794).

Similar cross section ratios plotted against the parent tube generation number are presented in figure 6, averaged for all lobes. The overall average for generations 6–17 is 0.82, in very good agreement with both the theoretically expected and the earlier experimental values. For the 6th–12th generations there seems to be quite a smooth wave of the ratio curve.

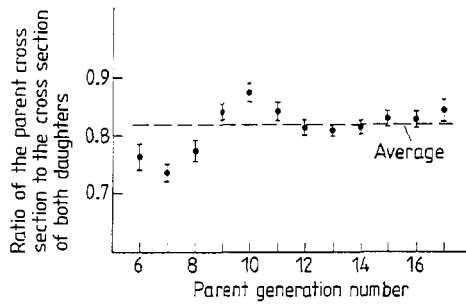


Figure 6. Ratios of parent tube cross sections to the total cross sections of both tubes.

Horsfield and Cumming also report that the minimum ratio they measured was about 0.4, i.e. there were cases (or at least one case) where the total cross section of both daughters exceeded double that of the parent tube cross section. We have also found such cases but the 37 observed cases out of the total 3704 bifurcations are negligible, or can simply be measurement or registration errors. The distribution of the cross section ratios averaged for all lobes for generations 6–17 is given in figure 7

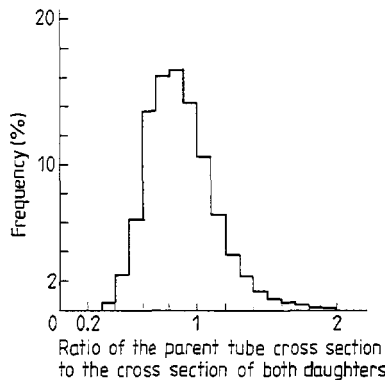


Figure 7. Distribution of the cross section ratios. The frequency is less than 0.5% for ratios greater than two.

and is to be used in step (4) of the selection process, to obtain the total cross section of the two daughters. The small deviation in the cross section ratios also demonstrates that, generally, greater diameter parents have greater diameter daughters.

The asymmetry of the branching can be characterised by the ratio of the diameters of the minor and major daughters of the same parents. Horsfield and Cumming found that in 27.6% of the cases the ratio is larger than 0.9, in 69% larger than 0.7 and the smallest value they found was 0.37. In our much larger data base the diameter ratio exceeds 0.9 in 36% of the cases, 0.7 in 82% and we have not found ratios below 0.4.

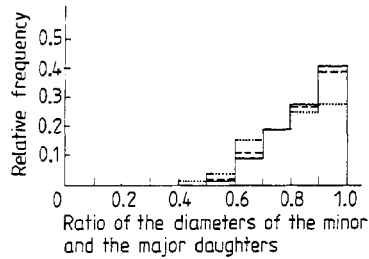


Figure 8. Distribution of the ratios of the diameters of the minor and major tubes of the same parents. Parent diameters: —, smallest 30%; ---, medium range; and ···, largest 30%.

The histogram in figure 8 shows the plausible result that high asymmetries (small ratios) are more frequent with relatively large diameter parent tubes. Figure 8 is to be used in step (4) for random distribution of the total diameter between major and minor daughters.

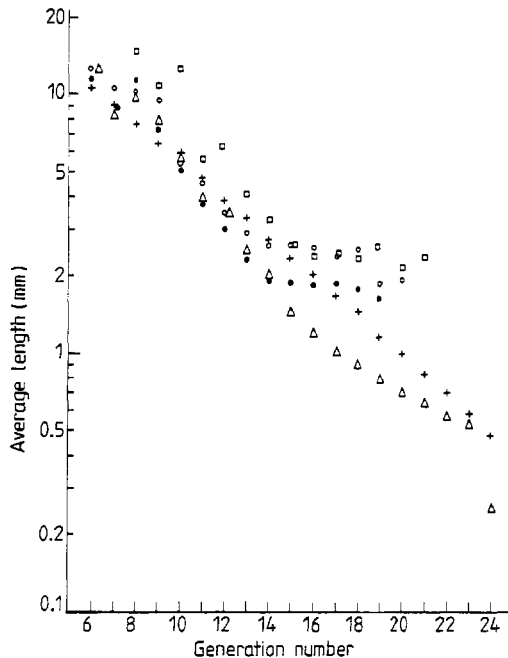


Figure 9. Average airway lengths plotted against generation numbers. In the comparison of the lengths plotted, especially at higher generation numbers, it should be borne in mind that in the deterministic models tubes from any given generation always have the same biological functions, whereas in the real casts analysed the tubes assigned to identical generation numbers are probably not at the same distance from terminal bronchioli. Symbols as given in figure 1.

7. Lengths of tubes, correlations with diameters

Average lengths of the tubes in the different generations are given in figure 9 for the same lobes as in figure 1 for the diameters. The distribution of the lengths within the generations is again near to log-normal. In figures 10(a) and 10(b) the averages and the relative standard deviations of the logarithms of lengths (in 0.1 mm) are again given.

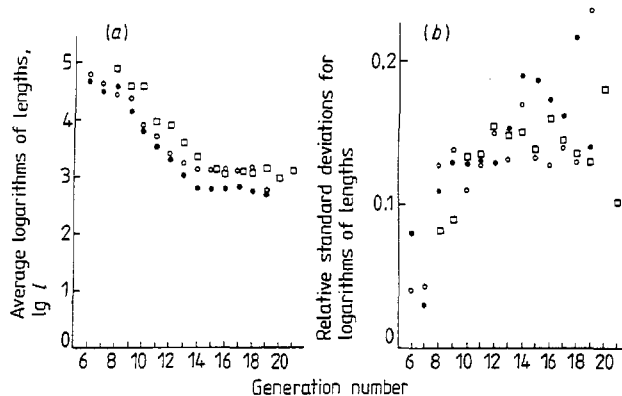


Figure 10. (a) Logarithms of lengths (where l is measured in 0.1 mm units) and (b) their relative standard deviations. Data taken from files: ●, DS1; ○, DS8; and □, DS10.

A major difference between the Lovelace ITRI data and the lengths used by Weibel or by Yeh and Schum is that in the Lovelace data there is again a 'saturation' effect, which in the case of lengths can hardly be explained by physical reasons. There is, however, a possible explanation—the cut off termination. Although the termination of the cast measurements is decided by diameter limits, if we assume that in general the narrower tubes are the shorter ones, then the lack of the shorter tubes at higher generation numbers becomes understandable.

The aim of the investigations presented here was precisely to find such correlations between the lengths and diameters of the tubes from the same generation of the same lobe. (This correlation substantially differs from the macrorrelation that higher generation tubes are shorter and narrower.)

All logarithms of tube diameters and lengths are tallied into seven equiprobability classes according to averages and standard deviations calculated for their own lobe and generation. It means that the range of the parameter investigated (e.g. diameter of tubes in the right upper lobe at generation 14) was divided into seven intervals in such a way that the same number of actual cases (one-seventh of the total) is expected to fall into each interval. The lowest interval is called class 1, the medium (where the near average values lie) is class 4, and the highest is called class 7. In this way every tube is classified by two integers: the diameter and the length classes; thus, the diameter-length relationship can be studied on data unified for all lobes and generations.

The next step is to construct a diameter class-length class matrix in such a way that every tube adds one to the matrix element determined by its diameter and length class values. The higher the correlation, the higher the values in the main diagonal. Instead of presenting a 7×7 matrix here, seven separate plots for the seven diameter classes are given in figure 11. It can be seen that in each case the most probable class number for length is the same as that for diameter.

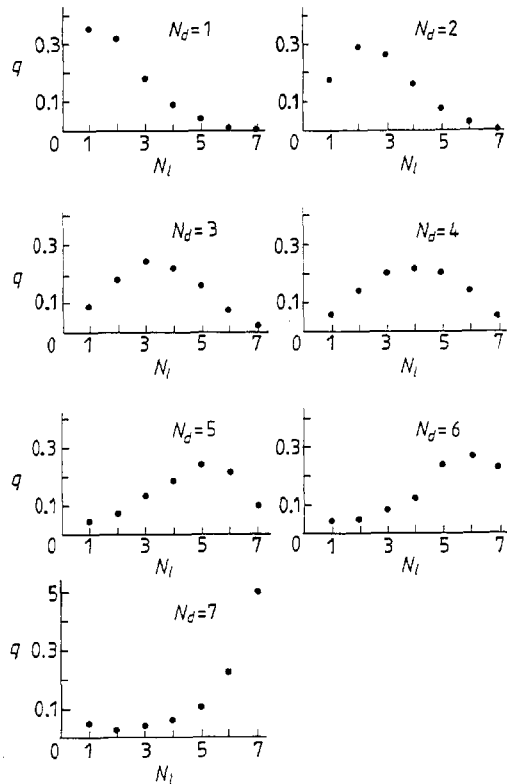


Figure 11. Correlations of the diameters and lengths of tubes of the same lobes and generations. q , relative frequency; N_d , diameter class number; N_l length class number.

Figure 11 is used to select the length in step (5) of the random geometry selecting process in the following way. First, by comparing the actual diameter of the tube investigated with the average and the deviation of its generation the class of diameter N_d to which the tube belongs is determined. Then, according to the probabilities given in the appropriate plot in figure 11 the length class is selected. Finally, the actual length is selected from the average length and standard deviation of the generation of the tube investigated and the class selected.

8. Branching angles

Branching angles (i.e. angles between daughter and parent tubes) are measured and registered to an accuracy of 5° . Our first investigation proved the well known observation that the major tubes generally have smaller branching angles than the minor ones. This relationship was found in about 60% of all cases; in 20% the minor daughter deviated from its parent less than the major one and in 20% the same angles were recorded for both daughters. With real, continuously varying structures, equality has zero probability; therefore the apparent equalities are caused by the rounding off to 5° . If we distribute the 'equal 20%' between larger major and minor daughter angles in the same ratio as we found in the non-equal cases then the final conclusion is that in 75% of the bifurcations the minor daughters have larger branching angles than their major sisters.

Besides the intentional rounding off mentioned earlier there seems to be a spontaneous one; the 'round' angles of 30° , 45° , 60° and 90° are much more frequently

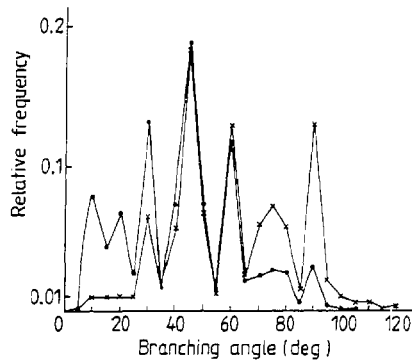


Figure 12. Relative frequencies of the recorded branching angles. ●, major tube; ×, minor tube.

recorded than other angles. This is clearly illustrated in figure 12 for generation 14 but similar plots can be drawn for all branching patterns. Since we do not believe that these angles are really distinguished, for the actual angle selection we intend to use distributions where the data for triplets of angles are used (e.g. data recorded for 40° , 45° and 50° are handled together as angles between 37.5° and 52.5°). In figures 13(a) and 13(b) the relative frequencies of finding branching angles less than 7.5° , 22.5° , 37.5° , 52.5° , 67.5° , 82.5° , 97.5° and 112.5° are plotted against the generation number, for the major and minor daughters respectively. (There are practically no branching angles above 97.5° for the major and below 7.5° for the minor daughters.) For the actual selections the probabilities given by the smooth full curves of figure 13 are to be used and linear interpolation is to be applied between the given angles, i.e. the cumulative distribution functions will be approximated by broken lines.

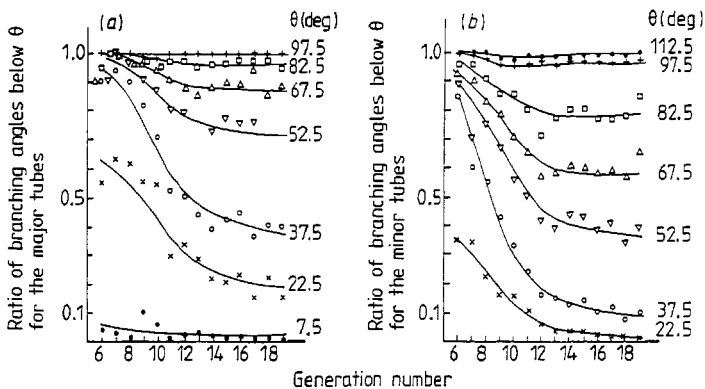


Figure 13. Probabilities of having branching angles below certain values θ plotted against generation number for (a) major and (b) minor tubes.

9. Gravity angles

Aerosol deposition is also influenced by the gravity angle, i.e. the declination of the tubes from the vertical. Unfortunately, gravity angles are recorded only for man B on the Lovelace ITRI files and those data are less than satisfactory for reliable statistical evaluation.

The gravity angles of first generations are well determined with small intersubject variations. The distribution may later be shown to become more and more uniform but from the very few data we have there seems to remain a downward preference

even at the highest generation numbers (averages published by Yeh and Schum 1980 also reflect such a tendency).

Thus, the validity of the hypothesis that the azimuth is uniformly distributed over $(0, 2\pi)$ at the bifurcations (at least for higher generation numbers) is not yet confirmed. If a more rigorous statistical evaluation of a larger data base later verifies the downward tendency, biasing will have to be applied.

10. Further tasks

In this paper a statistical analysis was presented on data recorded for lungs of two males. This means that our investigation was practically restricted to intrasubject variations; for a study of intersubject variations similarly careful measurements of many other lung casts are needed.

For the same reason statistical laws could be derived only for generations where the number of tubes was high enough. At the first, say, five generations (trivially, for the trachea) distributions can be estimated mainly by extrapolation from data of higher generations. Moreover the distributions may be different from those presented here. For example, the two main bronchi (generation 2) that lead to the right and left parts of the lung have well defined branching angles; no distribution like log-normal can be expected in this case.

The present discussion was restricted to problems of morphometry. The selection of the formulae describing deposition of aerosols at bifurcations with well defined but widely varying geometries has been investigated in many studies. The question of enhanced deposition at bifurcation sites (at carinal ridges) needs further investigation since the limited experimental data do not allow extrapolation to other aerosol diameters nor are there any theoretical formulae.

Acknowledgments

We are grateful to Dr Hsu-Chi Yeh, Lovelace ITRI for kindly sending us the magnetic tapes containing all the data that made the present study possible. The project was supported by the Hungarian Academy of Sciences and the Austrian Academy of Sciences.

Résumé

Analyse des données morphologiques du poumon humain pour l'application de méthodes stochastiques de calcul de dépôt des aérosols.

Les auteurs proposent un modèle pulmonaire stochastique pour le calcul du dépôt d'aérosols. La géométrie des voies aériennes est choisie aléatoirement, afin de refléter les variations, chez le même individu, du système respiratoire. Ce modèle peut également être ajusté pour prendre en compte les variations d'un individu à un autre. L'analyse statistique de la géométrie des voies aériennes humaines repose sur des données morphométriques obtenues au Lovelace Inhalation Toxicology Research Institute. Les auteurs présentent les valeurs moyennes et les distributions des diamètres et des longueurs des voies aériennes, les distributions des angles formés aux séparations bronchiques, ainsi que les critères choisis au niveau des terminaisons des voies aériennes (quand la région alvéolaire est atteinte). Les corrélations entre les sections transversales des tubes de générations successives et celles entre les diamètres et les longueurs d'une même génération sont également présentées.

Zusammenfassung

Die Analyse morphometrischer Daten der menschlichen Lunge für stochastische Berechnungen der Aerosolablagerungen.

Ein stochastisches Lungenmodell zur Berechnung von Aerosolablagerungen wird vorgestellt. Dabei wird die Geometrie der Luftwege nach dem Zufallsprinzip ausgewählt, um so die Schwankungen im System der Luftwege, sowie Schwankungen zwischen einzelnen Personen berücksichtigen zu können. Die statistische Analyse der verwendeten Geometrie für die menschlichen Luftwege basiert auf morphometrischen Daten, die am Lovelace Inhalation Toxicology Research Institute gemessen worden sind. Durchschnittswerte und Verteilungen des Durchmessers und der Länge der Luftwege, Verteilungen des Verzweigungswinkels sowie Kriterien zur Beendigung des Ablaufs (wenn die Alveolarregion erreicht ist) werden gegeben. Korrelationen zwischen den Röhrenquerschnitten nachfolgender Generationen sowie solche zwischen Durchmesser und Länge der gleichen Generation werden ebenfalls angegeben.

References

- Chan T L and Lippmann M 1980 *Am. Ind. Hyg. Assoc. J.* **41** 399
- D'Arcy Thompson W 1942 *Growth and Form* (Cambridge: Cambridge University Press)
- Hansen J E and Ampaya E P 1975 *J. Appl. Physiol.* **38** 990
- Heyder J, Gebhart J, Roth C, Stahlhofen W, Stuck B, Tarroni G, DeZaiacomo T, Formignani M and Melandri C 1978 *J. Aerosol Sci.* **9** 147
- Heyder J, Gebhart J and Stahlhofen W 1980 *Generation of Aerosols* ed. K Willeke (Ann Arbor, MI: Ann Arbor Science) pp65-103
- Hofmann W, Koblinger L, Daschil F, Fehér I and Balásházy I 1984 in *Recent Developments and New Trends in Radiation Protection* vol. 1 ed. E Tschirf and A Hefner (Vienna: ÖSV-Mitteilung) pp 250-7
- Horsfield K 1974 *Br. J. Dis. Chest.* **68** 145
- Horsfield K and Cumming G 1967 *Bull. Math. Biophys.* **29** 245
- 1968 *J. Appl. Physiol.* **24** 373
- Horsfield K, Dart G, Olson D E, Filley G F and Cumming G 1971 *J. Appl. Physiol.* **31** 207
- Lippmann M and Albert R E 1969 *Am. Ind. Hyg. Assoc. J.* **30** 257
- Phalen R F, Yeh H C, Schum G M and Raabe O G 1978 *Anat. Rec.* **190** 167
- Raabe O G, Yeh H C, Schum G M and Phalen R F 1976 *Tracheobronchial Geometry: Human, Dog, Rat, Hamster, LF-53, Lovelace Foundation Report*
- Soong T T, Nicolaidis P, Yu C P and Soong S C 1979 *Resp. Physiol.* **37** 161
- Stahlhofen W, Gebhart J and Heyder J 1981 *Am. Ind. Hyg. Assoc. J.* **42** 348
- Tarroni G, Melandri C, Prodi V, DeZaiacomo T, Formignani M and Bassi P 1980 *Am. Ind. Hyg. Assoc. J.* **41** 826
- Weibel E R 1963 *Morphometry of the Human Lung* (Berlin: Springer)
- Yeates D B and Aspin N 1978 *Resp. Physiol.* **32** 91
- Yeh H C 1984 private communication
- Yeh H C and Schum G M 1980 *Bull. Math. Biol.* **42** 461
- Yu C P and Diu C K 1982 *Aerosol Sci. and Techn.* **1** 355
- Yu C P, Nicolaidis P and Soong T T 1979 *Am. Ind. Hyg. Assoc. J.* **40** 999